

Lecture 3 - Collège de France - Spring 2013

Antoine Georges

(Dated: April 10, 2013)

Disclaimer: this is just a draft notebook... I am most grateful to Jernej Mravlje for his help in preparing these lecture notes. All possible mistakes are mine however...

I. HEIKES AND SHASTRY-KELVIN

A. General considerations

From $dE = \delta Q + \delta W = Tds + \mu dn$, the energy current reads: $j_E = Tj_s + \mu j_n$. Substituting this into the transport equations, one gets $j_E = L_{E,N}(-\nabla\mu) + L_{E,T}(-\nabla T)$ with:

$$L_{E,N} = TL_{21} + \mu L_{11} \quad , \quad L_{E,T} = TL_{22} + \mu L_{12} \quad (1)$$

Inverting these relations and using $L_{21} = L_{12}$, we can express the thermopower $\alpha = -L_{12}/eL_{11}$ as:

$$\alpha = -\frac{1}{T} \frac{L_{E,N}}{eL_{N,N}} + \frac{\mu}{eT} \quad (2)$$

Heikes approximation. At high- T , μ is linear in T and the first term is expected to behave as $1/T$ (loosely speaking, energy is bounded, cf Prelovsek).

$$\alpha_H = \frac{\mu}{eT} \quad (3)$$

Shastry-Kelvin approximation. Let us consider the density gradient given by:

$$\nabla n = \frac{\partial n}{\partial \mu}|_T \nabla \mu + \frac{\partial n}{\partial T}|_\mu \nabla T \quad (4)$$

Using the thermodynamic identity (note the minus sign !):

$$\frac{\partial n}{\partial T}|_\mu = -\frac{\partial n}{\partial \mu}|_T \frac{\partial \mu}{\partial T}|_n \quad (5)$$

one obtains:

$$\nabla n = \frac{\partial n}{\partial \mu}|_T \left[\nabla \mu - \frac{\partial \mu}{\partial T}|_n \nabla T \right] \quad (6)$$

and:

$$j_n = \left(\frac{\partial n}{\partial \mu}|_T \right)^{-1} (-\nabla n) + \left[L_{12} + L_{11} \frac{\partial \mu}{\partial T}|_n \right] (-\nabla T) \quad (7)$$

We observe that if we take $\alpha = \nabla \mu / e \nabla T = -L_{12}/eL_{11}$ to be:

$$\alpha_{SK} = \frac{1}{e} \frac{\partial \mu}{\partial T}|_n \quad (8)$$

we insure simultaneously $j_n = 0$ and $\nabla n = 0$. According to Shastry, this also follows from taking the ‘slow limit’ of the Kubo formula.

The two expressions are identical in the large- T limit, since then $\mu \propto T$. In order to make sense of the Heikes formula at lower- T , one needs a subtraction (e.g. $[\mu - \mu(0)]/T$).

Using thermodynamic identities:

$$\alpha_H = -\frac{1}{e} \frac{\partial S}{\partial n} \Big|_E, \quad \alpha_{SK} = -\frac{1}{e} \frac{\partial S}{\partial n} \Big|_T \quad (9)$$

These simple formula, although approximate, beautifully illustrate physical relation between the thermopower and the entropy per particle.

These formula are usually combined with an estimate of the entropy or chemical potential for an isolated atom, but turn out to be useful (and more accurate) in a broader context, especially for the SK formula. Namely, using an evaluation of $\mu(n, T)$ with more accurate means (e.g. DMFT). The (great) advantage is that a transport calculation is replaced by a simpler, thermodynamic calculation. Also, it gives intuition into the physics and the variation of the thermopower with T and n from the behaviour of entropy.

B. Single-orbital case: atomic limit

Useful references: Chaikin and Beni, PRB 13 (1976) 647; Kwak, Beni and Chaikin PRB 13 (1976) 641.

1. Two simple limits: $T \gg U$ and $T^* \ll T \ll U$

a. $T \gg U$ (i.e. one can set $U = 0$, electrons can be viewed as independent; for each spin direction, probability of occupancy p).

$|0\rangle$: $(1-p)^2$, $|\sigma\rangle$: $p(1-p)$, $|\uparrow\downarrow\rangle$: p^2 with $n/2 = p$, hence:

$$S/k_B = -2 \left[\frac{n}{2} \ln \frac{n}{2} + \left(1 - \frac{n}{2}\right) \ln \left(1 - \frac{n}{2}\right) \right], \quad \alpha = -\frac{1}{e} \frac{\partial S}{\partial n} = \frac{k_B}{e} \ln \frac{n}{2-n} \quad (10)$$

We observe (Fig. 1) that this diverges in the limit of a band insulator ($n = 0, n = 2$) and vanishes in the particle-hole symmetric case $n = 1$.

b. $T \ll U$ (i.e. one can set $U = \infty$). The analysis below is only valid however for $T \gg T^*$, with T^* the scale for metallic coherence, see below.

Only densities $0 \leq n \leq 1$ can be considered then.

$|0\rangle$: $1 - 2p$, $|\sigma\rangle$: p , $|\uparrow\downarrow\rangle$: 0 , with again $n = 2p$. Hence:

$$S/k_B = - \left[(1-n) \ln(1-n) + 2 \frac{n}{2} \ln \frac{n}{2} \right], \quad \alpha = -\frac{1}{e} \frac{\partial S}{\partial n} = -\frac{k_B}{e} \ln \frac{2(1-n)}{n} \quad (11)$$

In this case, we find a divergence when both the band ($n = 0$) and Mott ($n = 1$) insulators are reached (Fig. 1).

A similar analysis can be done for $1 \leq n \leq 2$, assuming that only states $|\sigma\rangle$ and $|\uparrow\downarrow\rangle$ are present and $|0\rangle$ is forbidden. This amounts to change n into $2 - n$ in the above expressions (particle-hole symmetry), leading to $\alpha = -k_B/e \ln 2(n-1)/(2-n)$.

2. Full calculation in the atomic limit

Partition function:

$$Z_G = 1 + 2e^{\beta\mu} + e^{-\beta(U-2\mu)} \equiv 1 + 2\xi + \xi^2 e_u \quad (12)$$

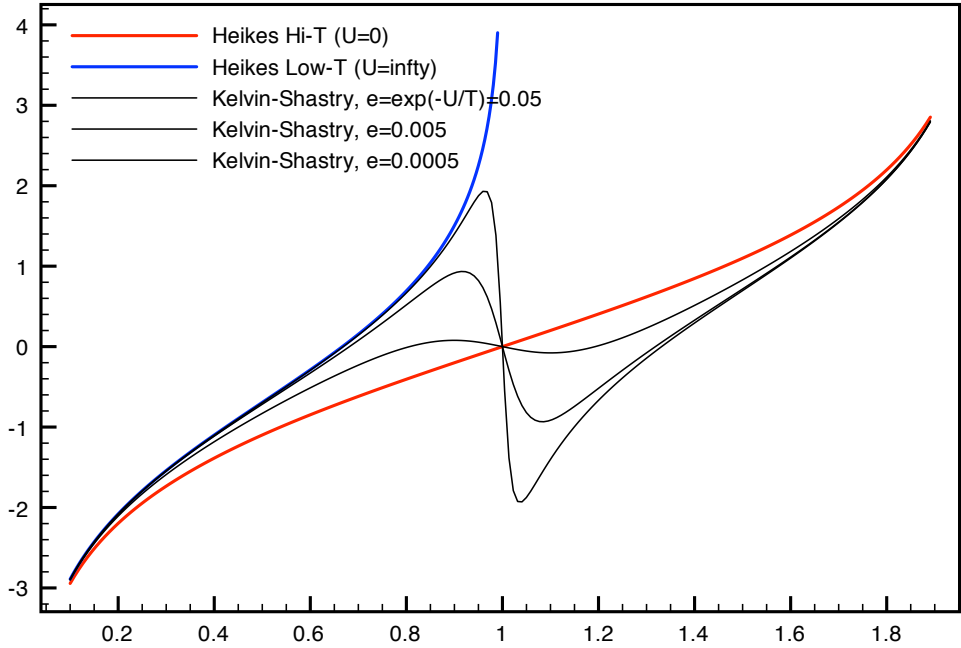


FIG. 1: Single-orbital Hubbard model: the two Heikes limit and generalized Kelvin-Shastry formula in the atomic limit

with the notations $\xi \equiv e^{\beta\mu}$ (fugacity) and $e_u \equiv e^{-\beta U}$.

Number of particles per site:

$$n = 2 \frac{\xi + \xi^2 e_u}{1 + 2\xi + \xi^2 e_u} \quad (13)$$

This relation can be inverted to yield:

$$\xi \equiv e^{\beta\mu} = \frac{R - (1 - n)}{(2 - n)e_u}, \quad R \equiv \sqrt{(1 - n)^2 + n(2 - n)e_u} \quad (14)$$

Note that this correctly yields $\mu = U/2$ ($\xi = 1/\sqrt{e_u}$) for $n = 1$ at all temperatures.

Using this into a generalized Heikes formula at finite- T raises some issues regarding the proper subtraction to be made, preserving particle-hole symmetry, etc...

In contrast, the Shastry-Kelvin approach yields a very reasonable result, at least qualitatively. Using $\partial\mu/\partial T = \ln \xi - (\partial \ln \xi / \partial \ln e_u) \ln e_u$, one obtains:

$$\frac{e}{k_B} \alpha_{SK} = \ln \frac{R - (1 - n)}{2 - n} - \frac{n(2 - n)e_u \ln e_u}{2R[R - (1 - n)]} \quad (15)$$

This expression is plotted as a function of density, for different values of T/U (different e_u 's) in Fig. 1. It nicely interpolates between the low- T and hi- T Heikes formulas, while preserving symmetry properties. Of course, at any finite- T , $\alpha(n)$ is a continuous function (although very steep close to commensurate filling levels at low- T). Note that the low- T ($U = \infty$) Heikes formula is only reached at very low- T (in this low- T regime the atomic limit approximation is usually no longer valid, so that in practice the validity of the low- T Heikes estimate is limited in the single-orbital case).

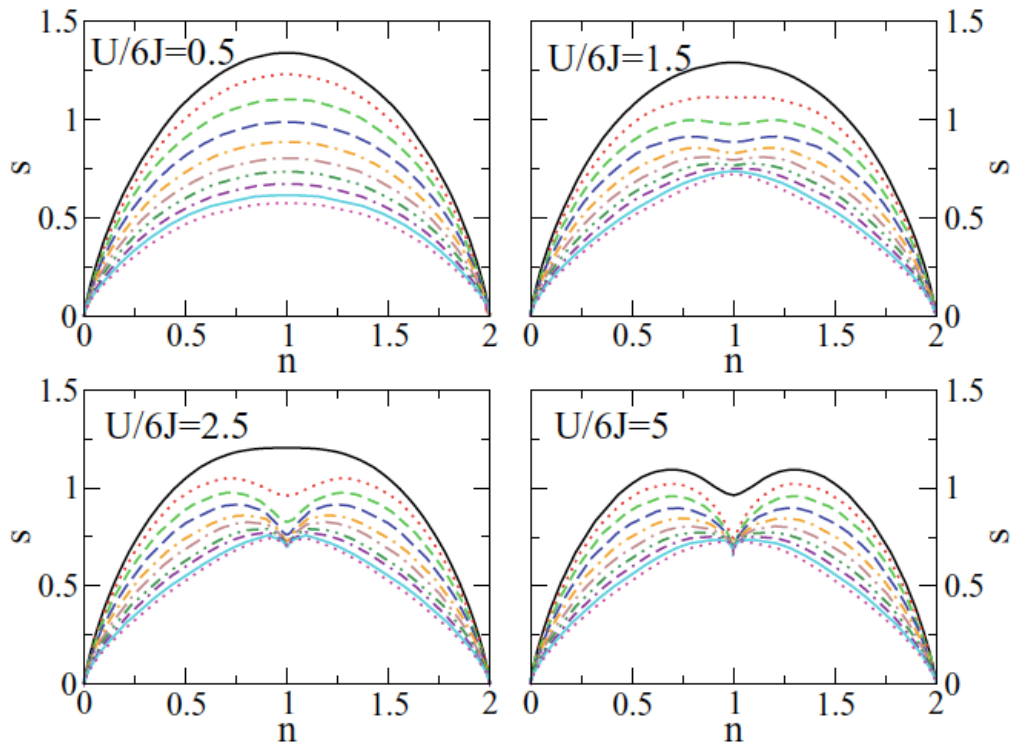


FIG. 2: Entropy of the single-band Hubbard model (cubic lattice) calculated by DMFT, in the high to intermediate temperature regime $\beta D = 1, \dots, 10$ (from De Leo et al. Phys Rev A 83, 023606 (2011)).

3. Physical understanding from entropic considerations

From Fig. 1, we see that at a given temperature, the density-dependence of the thermopower is non-monotonous. It passes through a maximum and also crosses zero. The characteristic doping levels at which this happens depend on T . This can be understood from the overall density-dependence of the entropy, since $\alpha_{SK} \propto -\partial S/\partial n$.

A (DMFT) calculation at relatively hi- T of the entropy vs. n is reproduced in Fig.2. For large U and $T \ll U$, the entropy is locked at the value $\ln 2$ corresponding to the spin-degeneracy of the paramagnetic Mott insulator. Upon doping, density fluctuations increase entropy beyond this value: entropy gets larger by doping away from the Mott insulator, and decreases again at low-density. Hence the non-monotonous behaviour and the corresponding zero-crossing of the thermopower (corresponding to the maximum of the entropy as a function of n).

4. Taking metallic coherence into account

At lower temperature, when metallic coherence (T^*) is reached, the entropy of the doped system becomes small again (because it is a degenerate Fermi system and entropy is proportional to T).

A quantitative calculation of the thermopower through this crossover requires more sophisticated techniques, such as DMFT combined with the Kubo formalism. This has been done by various authors (e.g. Deng et al. PRL 110, 086401 (2013), Arsenault et al. PRB 2013, Xu et al. PRB 2011).

We display on Fig. 3 the recent results of Deng et al. One point to be noted is the rather extended range of validity of the Shastry-Kelvin formula when $\partial\mu/\partial T$ is calculated exactly. Another approximate formula to which comparison can be made is the infinite-frequency limit (Shastry, Xu et al.).

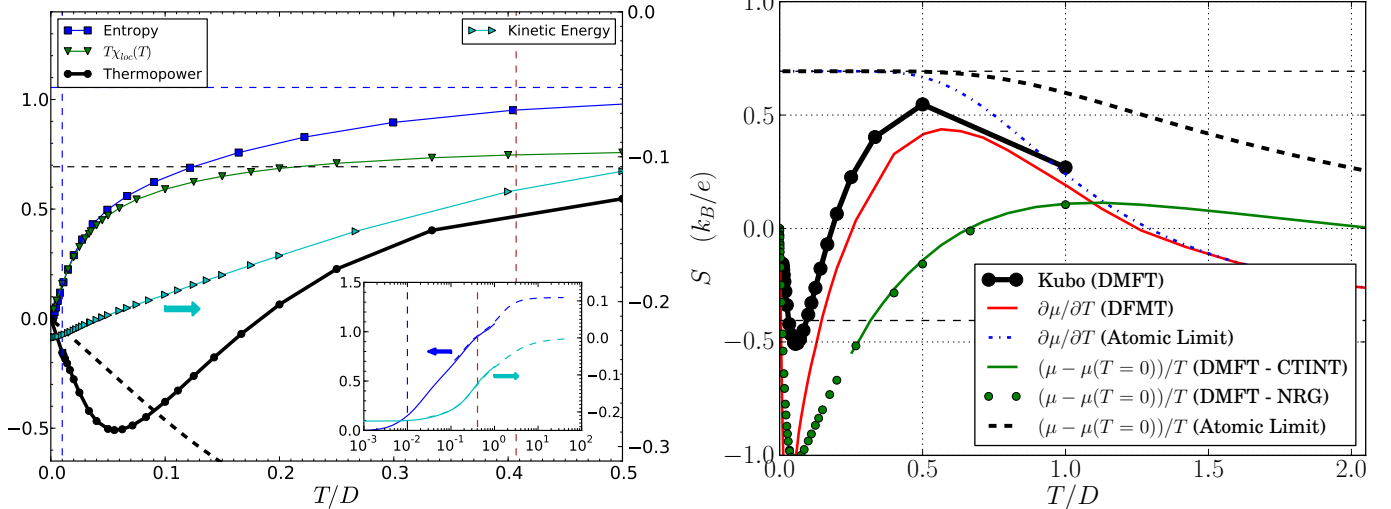


FIG. 3: Entropy and Seebeck coefficient calculated from DMFT-Kubo for a single-band Hubbard model $U/D = 4$, 20% hole-doping level. (Deng et al. PRL 110, 086401 (2013)). Note the crossover from the low- T metallic regime to the two Heikes regimes for $T^* < T < U$ and $T > U$. Note also the rather extended range of applicability of the Shastry-Kelvin formula when $\partial\mu/\partial T$ is calculated exactly.

Phenomenological description of the metallic crossover. At a phenomenological level, the crossover between a degenerate metal at low- T and the high- T Heikes formula can be captured by interpolating the entropy e.g. in the form:

$$S \simeq S_H(T, n) \tanh \frac{T}{T^* S_H} \quad (16)$$

in which we choose T^* such that the low- T behaviour of the entropy is reproduced ($T^* = 1/\gamma(n)$) - or we could also choose it so that in the end the correct value of the low- T slope of the thermopower independently calculated is reproduced. A key point is that $T^* \propto \delta D$ with $\delta = |1 - n|$ the doping level, reflecting the (Brinkman-Rice) enhancement of the effective mass as the Mott insulator is reached (and corresponding suppression of the coherence scale T^*).

The result of such an interpolation is displayed in Fig. 4. Compare to full DMFT calculation above.

C. Multi-orbital atom

The above analysis in the atomic limit can be generalized to a multi-orbital atom (M orbitals, maximum number of electrons n per atom is $2M$).

1. High- $T \gg U$ limit

In the high- T regime, we can consider independent electrons as above, with each quantum state $m\sigma$ having a probability $p = n/2M$ of being occupied. Hence the entropy and Heikes estimate:

$$S/k_B = -M \left[\frac{n}{2M} \ln \frac{n}{2M} + \left(1 - \frac{n}{2M}\right) \ln \left(1 - \frac{n}{2M}\right) \right] \quad (17)$$

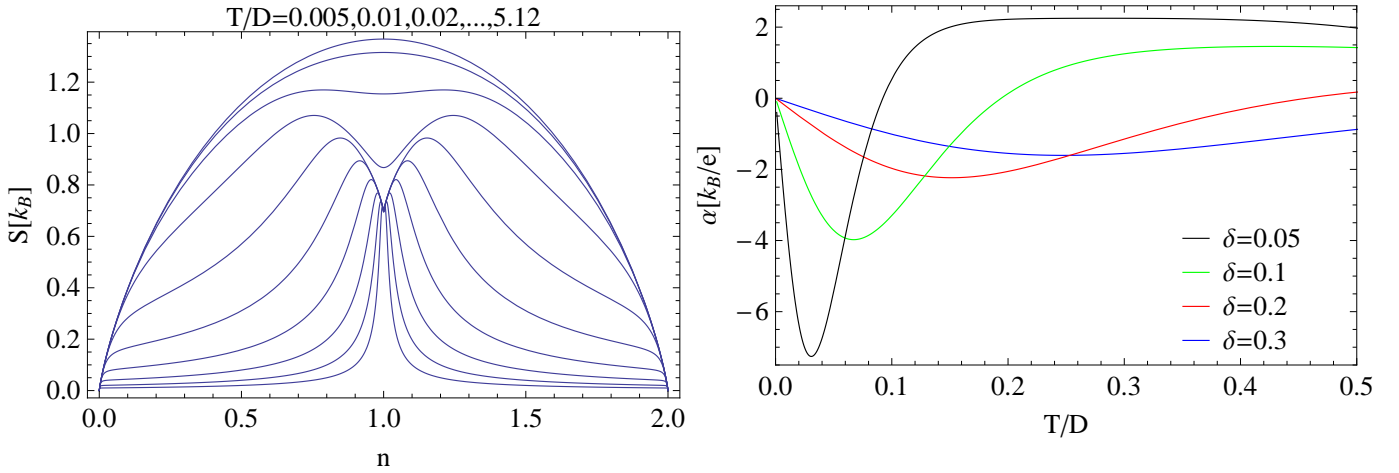


FIG. 4: Entropy and Seebeck from phenomenological interpolation.

$$\alpha_H = -\frac{k_B}{e} \ln \frac{2M-n}{n} \quad (18)$$

which again diverges only close to band insulators (Fig. 7).

2. $T \ll U$ regime

The general strategy is to use the grand-canonical partition function:

$$Z_G = \sum_{\Gamma} \exp -\beta(E_{\Gamma} - \mu N_{\Gamma}) = \sum_{\Gamma} \xi^{N_{\Gamma}} e^{-\beta E_{\Gamma}} \quad (19)$$

in which Γ labels all the atomic multiplets. The number of electrons per atom n and entropy are expressed in terms of the fugacity as:

$$n = \sum_{\Gamma} N_{\Gamma} p_{\Gamma} \quad , \quad S/k_B = -\sum_{\Gamma} p_{\Gamma} \ln p_{\Gamma} \quad , \quad p_{\Gamma} = \frac{1}{Z_G} \xi^{N_{\Gamma}} e^{-\beta E_{\Gamma}} \quad (20)$$

Eliminating ξ , one can obtain (numerically) $\mu(n, T)$ and $S(n, T)$ and from this the Heikes and Shastry-Kelvin estimates.

In the regime $T \ll U$ however, the dependence of n vs. μ displays a Coulomb staircase (Fig. 5), which allows one to simplify the analysis by focusing on a limited number of charge states. Retaining only three lowest-energy states in the $N-1, N, N+1$ sectors, the partition function and number of particles can be approximated as:

$$Z_G \simeq \xi^N [d_{N+1} e^{-\beta E_{N+1}} \xi + d_N e^{-\beta E_N} + d_{N-1} e^{-\beta E_{N-1}} \xi^{-1}] \quad (21)$$

$$n \simeq \frac{(N+1)d_{N+1} e^{-\beta E_{N+1}} \xi + N d_N e^{-\beta E_N} + (N-1)d_{N-1} e^{-\beta E_{N-1}} \xi^{-1}}{d_{N+1} e^{-\beta E_{N+1}} \xi + d_N e^{-\beta E_N} + d_{N-1} e^{-\beta E_{N-1}} \xi^{-1}} \quad (22)$$

Hence, the equation which determines the fugacity reads:

$$\xi^2 d_{N+1} e^{-\beta \Delta_{N+1}} [n - (N+1)] + \xi d_N [n - N] + d_{N-1} e^{-\beta \Delta_{N-1}} [n - (N-1)] = 0 \quad (23)$$

with $\Delta_{N\pm 1} \equiv E_{N\pm 1} - E_N$.

a. *Mixed valence* $N < n < N+1$. Then we can neglect the contribution from the $N-1$ sector, and we obtain:

$$\mu = k_B T \ln \left[\frac{d_N}{d_{N+1}} \frac{n - N}{N + 1 - n} \right] + E_{N+1} - E_N \quad (24)$$

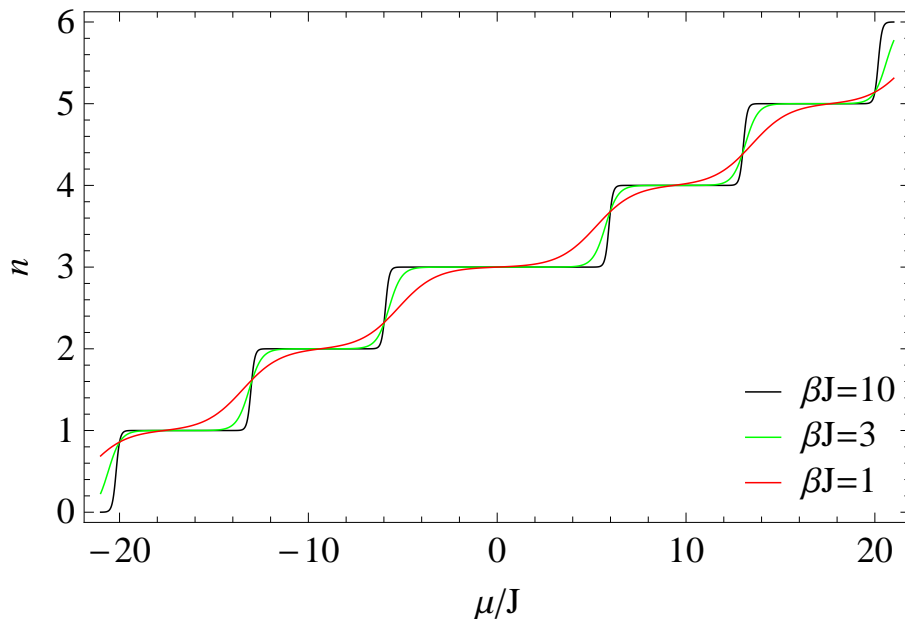


FIG. 5: Coulomb staircase, t_{2g} atom.

$$\alpha = \frac{k_B}{e} \ln \left[\frac{d_N}{d_{N+1}} \frac{n - N}{N + 1 - n} \right] \quad (25)$$

Now we see that this diverges close to the Mott insulating commensurate filling $n = N, N + 1$. Setting $n = N + x$, with x the (electron) doping level away from the filling- N insulator, we can rewrite:

$$\alpha = \frac{k_B}{e} \left[\ln \frac{d_N}{d_{N+1}} + \ln \frac{x}{1 - x} \right] \quad (26)$$

The first term corresponds to the entropy of spin-orbital degrees of freedom, and the second one to the entropy of doped electrons.

b. Integer filling $n = N$ Then the term linear in ξ vanishes, and we get:

$$\mu = \frac{1}{2} k_B T \ln \frac{d_{N-1}}{d_{N+1}} + \frac{E_{N+1} - E_{N-1}}{2} \quad (27)$$

$$\alpha = \frac{k_B}{e} \frac{1}{2} \ln \frac{d_{N-1}}{d_{N+1}} \quad (28)$$

Note that there are two sets of special values of the chemical potential, those corresponding to the mixed-valence steps (given by charge degeneracy points $E_N - \mu N = E_{N+1} - \mu_{N+1}$, hence $\mu = E_{N+1} - E_N$, and those corresponding to the integer charge plateaus $\mu = (E_{N+1} - E_{N-1})/2$. This is clearly apparent on Fig.6 displaying μ vs. T for a t_{2g} shell.

c. Interpolating formula from Shastry-Kelvin at finite T . As we did above for the single-orbital case, continuous curves for α as a function of density can be obtained from a full solution of the equations at finite- T (Fig. 7). However, in contrast to the scale U , we see that no dramatic suppression of α is induced when T reaches scale J (since we just feel other states then, but with the same charge, hence changes in μ are small).

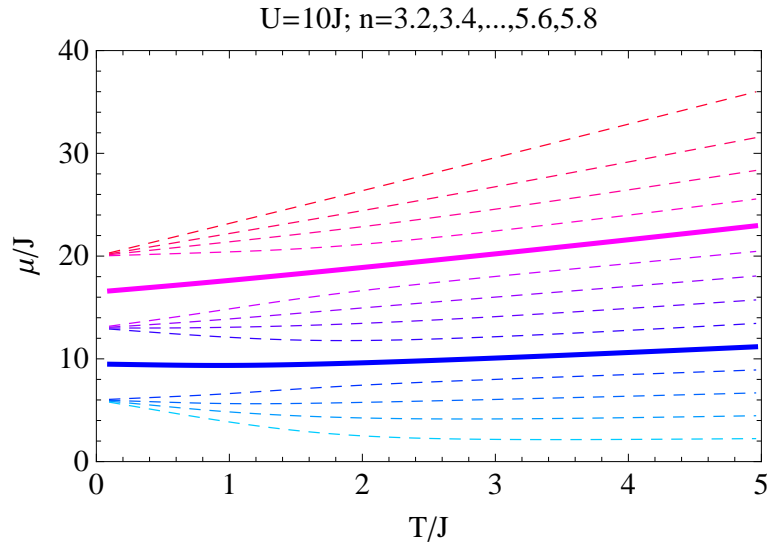


FIG. 6: Chemical potential vs. density, t_{2g} atom. Note that here $\mu = 0$ corresponds to the particle-hole symmetric case $n = 3$, i.e. μ has been shifted by $5(U - 3J)/2$.

D. Three orbitals in a t_{2g} shell

All these considerations are illustrated on the case of a t_{2g} shell with Kanamori interactions:

$$H = (U - 3J) \frac{\hat{n}(\hat{n} - 1)}{2} - 2J\mathbf{S}^2 - \frac{J}{2}\mathbf{L}^2 \quad (29)$$

The tables below give the eigenstates and degeneracies, as well as the relevant formulas for the thermopower. Those are plotted in Fig. 7 and Fig. 8

N	S	L	Degeneracy	Energy
0,[6]	0	0	1	$0, [15\mathcal{U}]$
1,[5]	1/2	1	6	$-5J/2, [10\mathcal{U} - 5J/2]$
2,[4]	1	1	9	$\mathcal{U} - 5J, [6\mathcal{U} - 5J]$
2,[4]	0	2	5	$\mathcal{U} - 3J, [6\mathcal{U} - 3J]$
2,[4]	0	0	1	$\mathcal{U}, [6\mathcal{U}]$
3	3/2	0	4	$3\mathcal{U} - 15J/2$
3	1/2	2	10	$3\mathcal{U} - 9J/2$
3	1/2	1	6	$3\mathcal{U} - 5J/2$

TABLE I: Eigenstates and eigenvalues of the t_{2g} Hamiltonian $\mathcal{U}n(n-1)/2 - 2J\mathbf{S}^2 - J\mathbf{L}^2/2$ in the atomic limit ($\mathcal{U} \equiv U - 3J$). The boxed numbers identifies the ground-state multiplet and its degeneracy, for $J > 0$. The multiplets within given charge are split by J . For $J = 0$, the degeneracies for $n = 2[4]$ is 15, and for $n = 3$ the degeneracy is 20. Other degeneracies are not influenced by J .

case	degeneracies ; $\alpha[k_B/e]$ for $T < J < U$	$J < T < U$
$n = 1$	1,9 ; $-\log[9]/2$	1,15 ; $-\log[15]/2$
$n = 2$	6,4 ; $\log[3/2]/2$	6,20 ; $-\log[10/3]/2$
$n = 3$	9,9; 0	15,15; 0
$0 < n < 1$	1,6 ; $-\log[(1-x)/x] - \log 6$;	1,6; $-\log[(1-x)/x] - \log 6$
$1 < n < 2$	6,9 ; $-\log[(1-x)/x] - \log 3/2$	6,15; $-\log[(1-x)/x] - \log 5/2$
$2 < n < 3$	9,4 ; $-\log[(1-x)/x] - \log 4/9$	15,20 - $\log[(1-x)/x] - \log 4/3$
$U < T$	$\log[\frac{2M-n}{n}]$	

TABLE II: Degeneracies and values of atomic Seebeck coefficient in different limits. Away from integer occupancies $n = N + x$, for integer N and $N < N + x < N + 1$, the last row is for the large $T \gg U$ for system with M orbitals.

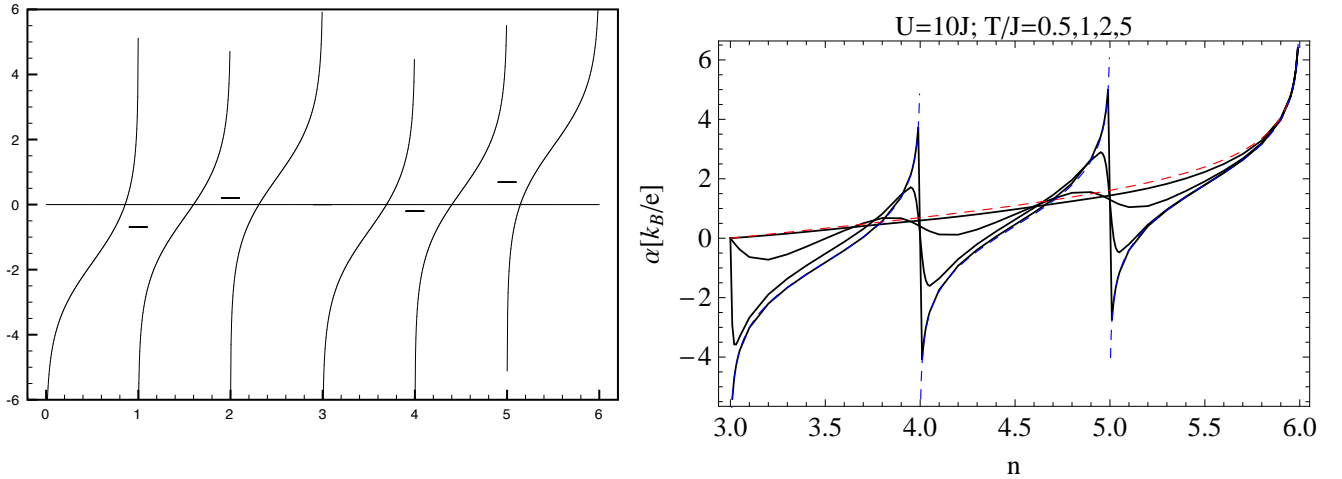


FIG. 7: Left: Seebeck coefficient vs. occupation of the shell for a t_{2g} system in the regime $T \ll J_H$. Horizontal bars indicate the values for integer filling. Right: Finite-temperature Shastry-Kelvin interpolation.

II. SEMI-CONDUCTING OXIDES: CASES WHERE HEIKES-KELVIN WORKS REASONABLY WELL

In some of the Mott insulating oxides which remain good insulators upon doping, the Heikes formula has been found to work, in some cases quantitatively. Some examples (see slides of lecture 3 and seminar by Sylvie Hébert):

- (Pr,Ca)CrO₃ and (La,Sr)CrO₃: d^3-d^2 . Pal et al. EPJB 53, 5 (2006), cf. figures in slides.
- (La,Sr)CoO₃: d^6-d^5

LaVO₃ [Uchida et al. PRB 83, 165127 (2011)] : qualitatively OK, not quantitatively though.

III. RUTHENATES AND OTHER METALLIC OXIDES: THE PUZZLE OF T-INDEPENDENT SEEBECK REGIME

See slides lecture 3

IV. THE COBALTATES: IS HEIKES APPLICABLE ? POSSIBLE ROLE OF FRUSTRATION

See seminar by S. Hébert.

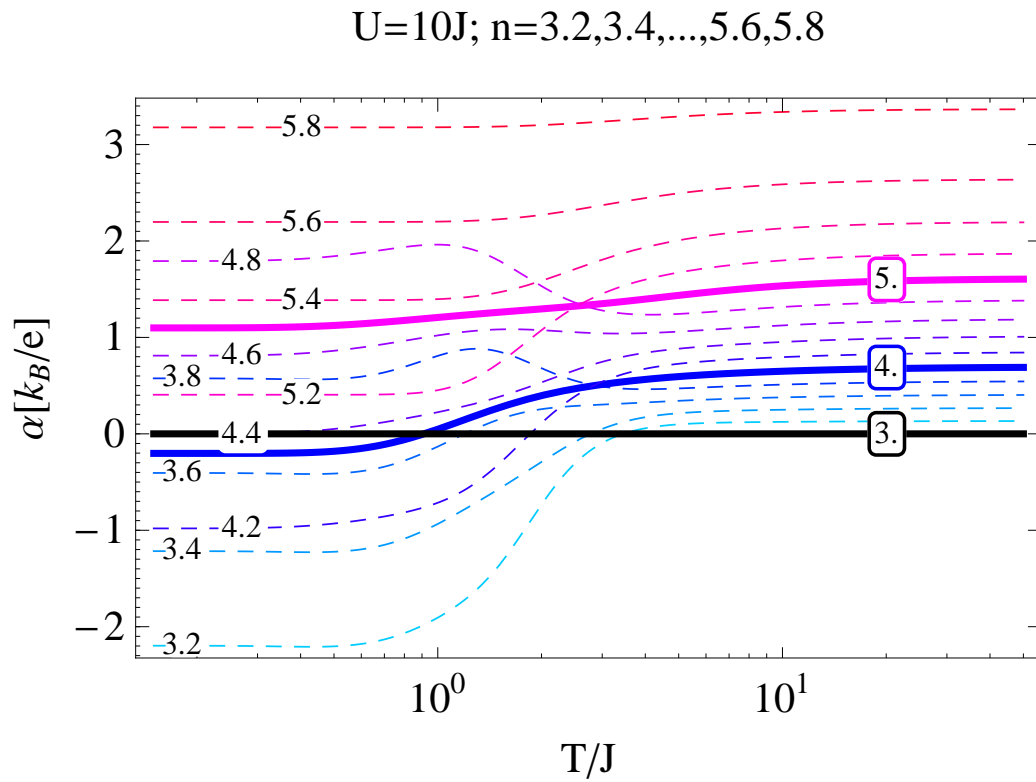


FIG. 8: Left: Seebeck coefficient vs. T/J for a t_{2g} atom.

V. THERMOPOWER AND ENTROPY: CUPRATES

See slides lecture 4.